

Complementary roles of initiation factor 1 and ribosome recycling factor in 70S ribosome splitting

Michael Y Pavlov, Ayman Antoun¹,
Martin Lovmar² and Måns Ehrenberg*

Department of Cell and Molecular Biology, BMC, Uppsala University, Uppsala, Sweden

We demonstrate that ribosomes containing a messenger RNA (mRNA) with a strong Shine–Dalgarno sequence are rapidly split into subunits by initiation factors 1 (IF1) and 3 (IF3), but slowly split by ribosome recycling factor (RRF) and elongation factor G (EF-G). Post-termination-like (PTL) ribosomes containing mRNA and a P-site-bound deacylated transfer RNA (tRNA) are split very rapidly by RRF and EF-G, but extremely slowly by IF1 and IF3. Vacant ribosomes are split by RRF/EF-G much more slowly than PTL ribosomes and by IF1/IF3 much more slowly than mRNA-containing ribosomes. These observations reveal complementary splitting of different ribosomal complexes by IF1/IF3 and RRF/EF-G, and suggest the existence of two major pathways for ribosome splitting into subunits in the living cell. We show that the identity of the deacylated tRNA in the PTL ribosome strongly affects the rate by which it is split by RRF/EF-G and that IF3 is involved in the mechanism of ribosome splitting by IF1/IF3 but not by RRF/EF-G. With support from our experimental data, we discuss the principally different mechanisms of ribosome splitting by IF1/IF3 and by RRF/EF-G.

The EMBO Journal (2008) 27, 1706–1717. doi:10.1038/emboj.2008.99; Published online 22 May 2008

Subject Categories: proteins

Keywords: IF1; initiation factors; protein synthesis; ribosome recycling factor; RRF

Introduction

When, in the bacterial cell, 70S ribosomes have finished messenger RNA (mRNA) translation, the completed proteins are released by the action of class-1 (RF1 and RF2) and class-2 (RF3) release factors (Freistroffer *et al*, 1997; Pavlov *et al*, 1997; Kisselev *et al*, 2003). Then, the post-termination ribosomes, still containing deacylated transfer RNA (tRNA) and mRNA, are split into subunits by ribosome recycling factor

(RRF) and elongation factor G (EF-G) in a GTP-dependent reaction (Janosi *et al*, 1996; Karimi *et al*, 1999; Peske *et al*, 2005; Zavialov *et al*, 2005b), which continuously supplies the cell with large (50S) and small (30S) ribosomal subunits for new rounds of initiation of mRNA translation. Initiation of bacterial protein synthesis normally proceeds through a 30S pre-initiation complex containing, apart from the 30S subunit, an mRNA, the initiator tRNA (fMet-tRNA^{fMet}) and the initiation factors 1 (IF1), 2 (IF2) and 3 (IF3) (Gualerzi and Pon, 1990). The first step in 30S pre-initiation complex formation after ribosome splitting by RRF and EF-G is the binding of IF3 to the 30S subunit, which induces dissociation of the deacylated tRNA and mRNA remaining from the previous round of protein synthesis (Karimi *et al*, 1999; Peske *et al*, 2005). The 30S pre-initiation complex, assembled by the subsequent binding of IF1 and IF2, a new mRNA and fMet-tRNA^{fMet} (Benne *et al*, 1973; Gualerzi and Pon, 1990; Antoun *et al*, 2006b), forms a 70S initiation complex ready for protein elongation by rapid docking to the 50S subunit (Benne *et al*, 1973; Antoun *et al*, 2006b). Accordingly, regular splitting of the 70S ribosome into subunits during protein synthesis occurs when it is in the post-termination state with an mRNA and a deacylated tRNA in the P site. However, due to aberrant events in protein synthesis and cellular responses to various stress situations, splitting into subunits of other than post-termination ribosomes is essential for the living cell.

When, for instance, ribosomes are stalled on truncated mRNAs (Singh and Varshney, 2004) or by the presence of antibiotic drugs (Tenson *et al*, 2003), peptidyl-tRNA drop-off (Menninger, 1976) may generate tRNA-free 70S·mRNA complexes. Such complexes may also be generated through the drop-off of peptidyl-tRNAs with short peptides at early stages of translation of specific mRNA sequences (Heurgue-Hamard *et al*, 2000; Gonzalez de Valdivia and Isaksson, 2005) or by premature docking of 50S subunits to 30S pre-initiation complexes lacking initiator tRNA (Antoun *et al*, 2006b).

Furthermore, when bacteria enter stationary phase or experience cold shock, superfluous ribosomes become stored either as inactive 70S ribosomes in complex with the YfiA protein (Vila-Sanjurjo *et al*, 2004; Ueta *et al*, 2005) or as inactive 100S dimers in complex with the RMF and YhbH proteins (Ueta *et al*, 2005). Such ribosomes need to be rapidly activated in response to improved growth conditions (Ueta *et al*, 2005).

Here, we demonstrate how the addition of IF1 together with IF3 and an mRNA containing a 'strong' Shine–Dalgarno (SD) sequence increased dramatically the rate of ribosome splitting into subunits, suggesting mRNA binding followed by the combined action of IF1 and IF3 as the dominant intracellular pathway for the splitting of tRNA-less ribosomes. Ribosome splitting by RRF and EF-G was, in contrast, slowed

*Corresponding author. Department of Cell and Molecular Biology, Biomedical Center, Uppsala University, Box 596, Husargatan 3, Uppsala 751 24, Sweden. Tel.: +46 18 471 4213; Fax: +46 18 471 4262; E-mail: ehrenberg@xray.bmc.uu.se

¹Present Address: Institute for Cancer Studies, University of Birmingham, Birmingham, UK

²Present Address: CMB/Microbiology, University of Gothenburg, Gothenburg, Sweden

Received: 22 February 2008; accepted: 28 April 2008; published online: 22 May 2008

down by the presence of an mRNA alone, but greatly accelerated by the presence of *both* an mRNA and a deacylated tRNA. In this latter case, the ribosomal splitting by IF1/IF3 was virtually blocked. Taken together, our data show that IF1/IF3- and RRF/EF-G-dependent splitting of different ribosomal complexes were complementary, that is, a complex rapidly split by IF1/IF3 was slowly split by RRF/EF-G and vice versa.

We have also found IF3 to be involved in the mechanism of IF1/IF3-dependent but not in the mechanism of RRF/EF-G-dependent ribosome splitting, and that the splitting of post-termination-like (PTL) ribosomes by RRF/EF-G was strongly affected by the identity of the deacylated tRNA in the P site. These and other data are used to discuss the different mechanisms of ribosome splitting into subunits by IF1 and IF3 on the one hand and by RRF and EF-G on the other.

Results

Complementarity of IF1/IF3 and RRF/EF-G in splitting of ribosomal complexes

We used an *in vitro* system for protein synthesis with *Escherichia coli* components of high activity and purity (Pavlov *et al*, 1997) to study the splitting of various ribosomal complexes into subunits with stopped-flow techniques in combination with monitoring of Rayleigh light scattering (Antoun *et al*, 2006b). The splitting reactions were normally monitored in the presence of IF3, which rapidly binds to dissociated 30S subunits and inhibits their re-association to free 50S subunits (Grunberg-Manago *et al*, 1975). The experiments are shown in Figure 1 and the estimated rate constants for the splitting of various ribosomal complexes are compiled in Table I.

The rate constant, q , for the dissociation of vacant 70S ribosomes was estimated as 0.003 s^{-1} (Figure 1A), and remained unaltered to changes in IF3 concentration above $1\text{ }\mu\text{M}$ (data not shown). Pre-incubation of 70S ribosomes with mXR7 mRNA (mXR7) (Table II) with a strong SD sequence before addition of IF3 or simultaneous addition of IF3 and mXR7 to the vacant ribosomes increased q by about an order of magnitude to 0.029 or 0.023 s^{-1} , respectively. When, instead, the 70S ribosomes were pre-incubated with mBar mRNA (mBar) (Table II) with a weak SD sequence before addition of IF3, there was only a two-fold increase in q (Figure 1A and Table I). Pre-incubation of the 70S ribosomes with only deacylated tRNA^{Phe} did not alter q (data not shown), but pre-incubation with both tRNA^{Phe} and mXR7 decreased q to virtually zero (Figure 1A). These observations suggest that, by itself, the SD-anti-SD (ASD) interaction between the mRNA leader and 16S rRNA decreased the affinity of ribosomal subunit binding, whereas this affinity was greatly increased by the simultaneous presence of an mRNA and a P-site-bound deacylated tRNA.

Addition of both IF3 and IF1 to vacant ribosomes, or to 70S ribosomes pre-incubated with either mXR7 or mBar (Figure 1B) resulted in an about 25-fold faster splitting, than when only IF3 was added to the same ribosomal complexes (Figure 1A and Table I). We note that the IF1/IF3-dependent splitting of ribosomes pre-incubated with mXR7 was remarkably fast (0.92 s^{-1}) and that splitting of vacant ribosomes by the simultaneous addition of IF1, IF3

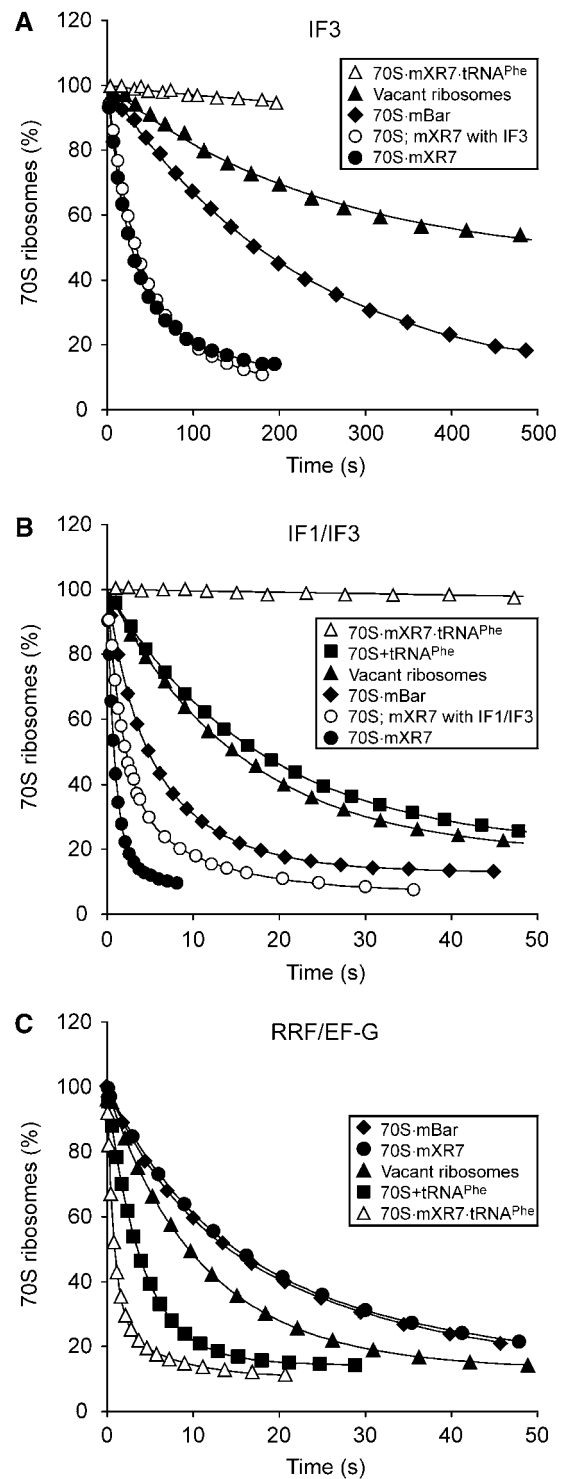


Figure 1 Splitting of 70S ribosomes and their complexes with mRNA and tRNA^{Phe} by IF3, by IF1 and IF3 or by RRF, EF-G and IF3. The mixtures from syringe 1 of the stopped-flow instrument were rapidly mixed with equal volumes of the mixture from syringe 2 containing (A) $2\text{ }\mu\text{M}$ IF3, (B) $2\text{ }\mu\text{M}$ IF3 and $5\text{ }\mu\text{M}$ IF1 or (C) $2\text{ }\mu\text{M}$ IF3, $9\text{ }\mu\text{M}$ RRF and $4\text{ }\mu\text{M}$ EF-G. Syringe 1 contained $0.3\text{ }\mu\text{M}$ vacant 70S ribosomes (\blacktriangle); $0.3\text{ }\mu\text{M}$ 70S ribosomes pre-incubated with $0.5\text{ }\mu\text{M}$ mXR7 mRNA (\bullet), with $0.5\text{ }\mu\text{M}$ mBar mRNA (\blacklozenge), with $0.5\text{ }\mu\text{M}$ deacylated tRNA^{Phe} (\blacksquare), with both mXR7 mRNA and tRNA^{Phe} (\triangle) or $0.3\text{ }\mu\text{M}$ 70S ribosomes but with mXR7 mRNA added in syringe 2 (\circ). All mixtures were prepared in LS4 buffer containing 4 mM free Mg^{2+} . All concentrations in the figure legends are given as final concentrations after the mixing.

Table I Splitting rate q (s^{-1}) of different ribosomal complexes in the presence of IF3, IF3 and IF1, or IF3 and RRF/EF-G

	IF3	IF3 + IF1	IF3 + RRF + EF-G
70S only	0.003 ± 0.006	0.063 ± 0.002	0.095 ± 0.005
70S + tRNA ^{Phe}	0.003 ± 0.007	0.057 ± 0.002	0.23 ± 0.01
70S + mXR7	0.029 ± 0.002	0.92 ± 0.04	0.064 ± 0.004
70S + mBar	0.006 ± 0.001	0.16 ± 0.02	0.068 ± 0.004
70S + mXR7 + tRNA ^{Phe}	~0	~0	1.05 ± 0.05
70S only; mXR7 with factors ^a	0.023 ± 0.002	0.53 ± 0.03	—

The sequences of mXR7 and mBar mRNAs are shown in Table 2. All experiments were conducted at 37°C in LS4 buffer containing 4 mM Mg²⁺. ^amXR7 mRNA was added together with IF3 or with IF1 and IF3.

Table II Complete sequences of synthetic mRNAs

mRNA	Complete sequence of mRNA
mXR7	GggAAUUCGGGCCUUGUUAACA UUUAAGGAGGU AUACU <u>AUGUUUACGAUUU</u> aaUUGCAGaaaaaaaaaaaaaaaaaaaaa
mBar	GggAAGCUGAACGAGAAACGUAAA <u>AUGUUCACGAUUU</u> aataAUCAAUAUACUGCAGaaaaaaaaaaaaaaaaaaaaa
mXR8	GggAAUUCGGGCCUUGUUAACA UUUAAGGAGGU AUACU <u>AUGUUCACGAUC</u> uaaUCUGCAGaaaaaaaaaaaaaaaaaaaaa
mXR8_FM	GggAAUUCGGGCCUUGUUAACA UUUAAGGAGGU AUACU <u>UUCAUGACGAUC</u> uaaUCUGCAGaaaaaaaaaaaaaaaaaaaaa
mSD022	GggAAUUCAAAA UUU AAAAGUUAAC AGGU AUACAUCU <u>AUGUUUACCAUUU</u> aaUCTGCAGaaaaaaaaaaaaaaaaaaaaa

mXR7, mXR8 and mXR8_FM mRNAs (Antoun *et al*, 2006b) with the upstream sequence similar to that of 002 mRNA (La Teana *et al*, 1993) had a strong UAAGGAGGU SD sequence marked in bold. mSD022 mRNA with the upstream sequence identical to that of 022 mRNA (La Teana *et al*, 1993) had a weak AGGU SD sequence (in bold). mBar mRNA with the upstream sequence identical to that of barI mRNA (Ontiveros *et al*, 1997) had a scrambled SD sequence AACGAG (in bold). Phenylalanine codons are marked as underlined bold while the initiation codons (canonical and non-canonical) as underlined italic. All mRNAs except mXR8_FM had MFT1 coding sequence. mXR8_FM mRNA had the MTI coding sequence.

and mXR7 was significantly slower ($0.53 s^{-1}$) but still sufficiently fast to be of physiological relevance (Figure 1B and Table I). Pre-incubation of 70S ribosomes with deacylated tRNA^{Phe} slightly reduced the rate of their splitting by IF1/IF3, whereas the pre-incubation with both mXR7 and tRNA^{Phe} reduced the splitting rate to virtually zero (Figure 1B and Table I).

Simultaneous addition of RRF, EF-G and IF3 to vacant ribosomes increased their splitting rate about 30-fold over that in the absence of RRF and EF-G (Table I). The splitting rates of 70S ribosomes pre-incubated with only tRNA^{Phe}, only mXR7 or both tRNA^{Phe} and mXR7 were significantly larger, moderately smaller or greatly larger, respectively, than when RRF, EF-G and IF3 were added to vacant ribosomes (Figure 1C and Table I).

Comparison of Figure 1B and C reveals that the splitting of ribosome complexes by RRF/EF-G on the one hand and by IF1/IF3 on the other were complementary. In other words, the most rapid splitting by RRF/EF-G occurred for ribosomes in complex with both mXR7 and tRNA^{Phe} (Figure 1C), where the splitting by IF1/IF3 was negligible (Figure 1B) and the most rapid splitting by IF1/IF3 occurred for ribosomes in complex with only mXR7 (Figure 1B), where the splitting by RRF/EF-G was the slowest (Figure 1C).

Concentration dependencies of IF1/IF3- and RRF/EF-G-induced ribosome splitting

The total concentrations of IF1, RRF and EF-G in the *E. coli* cytoplasm have been estimated to be about 10 μM (Howe and Hershey, 1983), 20 and 20 μM, respectively, (Andersen *et al*, 1999; Seo *et al*, 2004), but their free concentrations are unknown. To study how the rate of ribosome splitting by IF1/IF3 or by RRF/EF-G depends on the concentration of these factors at a fixed concentration of IF3, we performed IF1 titrations, RRF titrations at a fixed EF-G concentration and EF-G titrations at a fixed RRF concentration.

Figure 2A shows how the apparent splitting rate, Q , and the extent of splitting of vacant ribosomes by IF1/IF3 increased with increasing IF1 concentration. The actual rate constant, q , for ribosome splitting, was calculated according to the equation:

$$q = Q \frac{1 - f_{eq}}{1 + f_{eq}} \quad (1)$$

where f_{eq} is the fraction of non-dissociated 70S ribosomes in equilibrium (see Materials and methods). The increase in q was hyperbolic with a K_M value ($K_{M(IF1)}$) of 22 μM and a maximal rate q_{cat} ($q_{cat(IF1)}$) of $0.34 s^{-1}$ (Figure 2C and Table III).

When the 70S ribosomes were pre-incubated with mXR7 mRNA with a strong SD sequence before addition of IF3 at a fixed and IF1 at a varying concentration (Figure 2B), the maximal rate $q_{cat(IF1)} = 1.3 s^{-1}$ of ribosome splitting was much larger and $K_{M(IF1)} = 1.8 μM$ much smaller than for vacant ribosomes (Figure 2C and Table III).

The rate constant, q , for vacant ribosome splitting by EF-G at a fixed (3 μM) and RRF at a varying concentration in the presence of IF3 (1 μM), calculated from the apparent rate, Q , of the ribosomal splitting in Figure 3A, increased hyperbolically with the RRF concentration with a q_{cat} value ($q_{cat(RRF)}$) of $0.18 s^{-1}$ and a K_M value ($K_{M(RRF)}$) of 3.2 μM (Figure 3C and Table III). When the same type of titration experiment with EF-G fixed at 3 μM and RRF at a varying concentration was conducted with the ribosomes pre-incubated with mXR7 and tRNA^{Phe} (Figure 3B), we obtained $q_{cat(RRF)} = 1.7 s^{-1}$ and $K_{M(RRF)} = 9.8 μM$ (Figure 3C and Table III).

When, instead, vacant ribosome splitting was studied with RRF at a fixed (5 μM) and EF-G at a varying concentration (Figure 3D), a K_M value ($K_{M(EF-G)}$) of 2.8 μM and a k_{cat} value ($q_{cat(EF-G)}$) of $0.2 s^{-1}$ for the splitting reaction were obtained (Figure 3F). After pre-incubation of ribosomes with mXR7 mRNA and deacylated tRNA^{Phe}, we obtained $q_{cat(EF-G)} =$

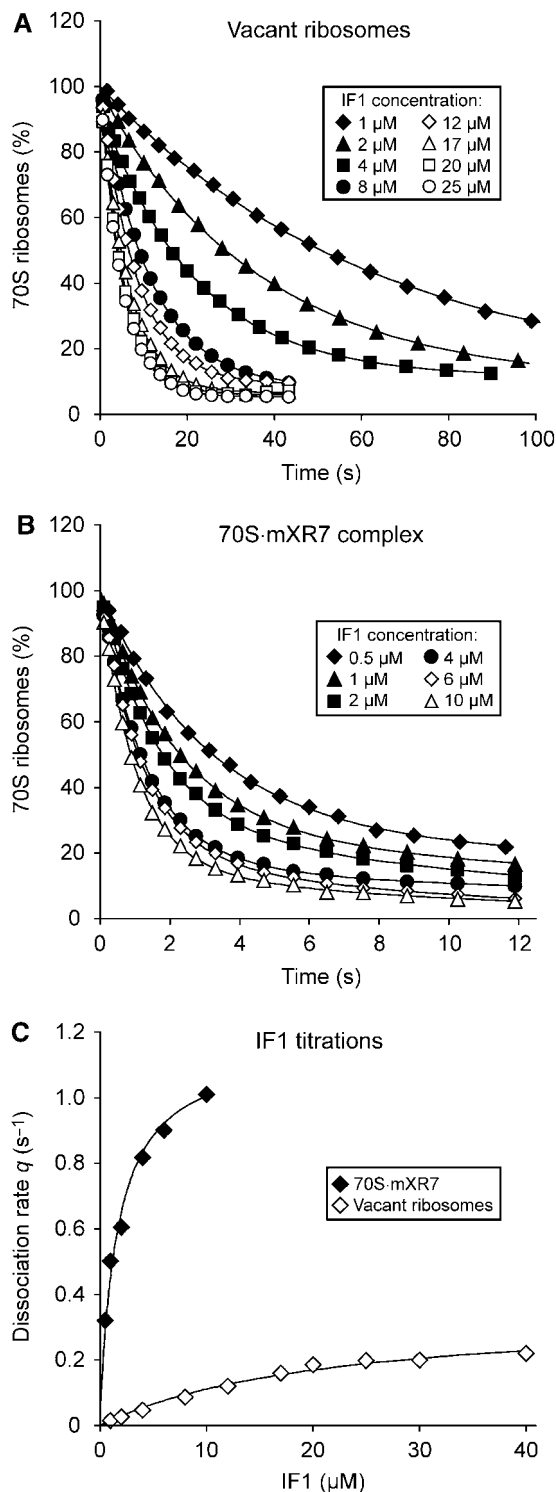


Figure 2 Effect of IF1 concentration on the rate of the IF1/IF3-induced splitting of vacant ribosomes and 70S·mRNA complexes. (A) Vacant 70S ribosomes (0.3 μM) or (B) 70S ribosomes (0.3 μM) pre-incubated with 0.5 μM mXR7 mRNA were rapidly mixed with the mixture containing 2 μM IF3 and different concentrations of IF1. All mixtures were prepared in LS4 buffer. (C) The splitting rate q was plotted versus IF1 concentration and fitted to the Michaelis–Menten equation: $q = q_{\text{cat}}[\text{IF1}]/([\text{IF1} + K_M])$.

0.8 s^{-1} and the $K_{M(\text{EF-G})} = 0.9 \text{ μM}$ from a similar titration experiment (Figure 3E and F). The different values of $q_{\text{cat}(\text{RRF})} = 1.7 \text{ s}^{-1}$ and $q_{\text{cat}(\text{EF-G})} = 0.8 \text{ s}^{-1}$ obtained for the 70S·mXR7·RNA^{Phe} complex are explained by the near-

saturation of EF-G concentration in the RRF titration experiment and the sub-saturating RRF concentration in the EF-G titration experiment.

Role of IF3 in IF1/IF3-induced ribosome splitting

Dissociation of 70S ribosomes into 30S and 50S subunits can be described by the scheme:



Here, q and k are compounded rate constants for the dissociation (q) and association (k) of the 30S and 50S subunits, which depend on the presence and concentrations of IFs, mRNA and other factors (Grunberg-Manago *et al*, 1975). Subunit association experiments shown in Figure 4A demonstrate that the addition of IF1 (up to 15 μM) resulted in a small increase (from 3.6 to 5.4 μM⁻¹s⁻¹) in k for the association of vacant subunits and in a slight decrease (from 2.1 to 1.8 μM⁻¹s⁻¹) in k for the association of 30S·mRNA complexes to 50S subunits. Earlier experiments with vacant ribosomes demonstrated that the addition of IF3 greatly decreased k but left q virtually unaltered (Grunberg-Manago *et al*, 1975). If one assumes that IF3 does not affect q also in the presence of IF1 one can estimate the expected equilibrium dissociation constant $K_d = q/k$ in the absence of IF3 for different IF1 concentrations using the values of k measured in experiments in Figure 4A and values of q measured in experiments in Figure 2. Taking values $k \sim 1.8 \text{ μM}^{-1} \text{ s}^{-1}$ and $q \sim 1 \text{ s}^{-1}$ measured at 15 μM IF1 one gets $K_d \sim 0.6 \text{ μM}$, which would imply that a considerable dissociation of 70S·mRNA complexes should occur at this IF1 concentration even in the absence of IF3.

Figure 4B shows, in contrast, that without IF3 the extent of dissociation of 0.2 μM 70S·mXR7 complex by 15 μM IF1 was not the 80% expected from the K_d value of 0.6 μM but only 20%, which corresponds to the K_d value of about 0.01 μM (Equation (7) in Materials and methods). This 60-fold discrepancy between the expected and measured K_d values indicates that the rate constant q of 70S·mXR7 splitting by IF1 was greatly affected by IF3, which implies a direct interaction of IF3 with the 70S·mRNA IF1 complex. This conclusion is further validated by the comparison of the q value of 1 s⁻¹ measured in the presence of both IF1 and IF3 (Figure 4B) with the q value of 0.018 s⁻¹ calculated according to Equation (1) from the f_{eq} value of 0.8 and the apparent rate Q of 0.16 s⁻¹ measured for 70S·mRNA splitting by IF1 alone (Figure 4B). The extent of vacant ribosome dissociation by 20 μM IF1 was small (Figure 4B), making the precision of the K_d and q estimates low. We could, however, estimate the upper bound for q ($< 0.006 \text{ s}^{-1}$) in the absence of IF3 from the fraction ($f_{\text{eq}} \sim 0.93$) of remaining 70S ribosomes and the apparent splitting rate Q ($\sim 0.14 \text{ s}^{-1}$). In the presence of IF3, in contrast, we estimated q as 0.15 s⁻¹ (Figure 2A). This implies an at least 20-fold increase in the rate q of IF1-dependent splitting of vacant ribosomes by IF3, which shows that IF3 interacts directly not only with the 70S·mRNA·IF1 but also with the 70S·IF1 complex and promotes their splitting into subunits (see Discussion).

Table III q_{cat} and K_M parameters for the splitting of ribosomal complexes by IF1/IF3 and RRF/EF-G

Splitting with	Titration with	Complex	q_{cat} (s^{-1})	K_M (μM)
IF1/IF3	IF1 (IF3 = 2 μM)	Vacant ribosome	0.34 ± 0.05	22 ± 4
IF1/IF3	IF1 (IF3 = 2 μM)	70S:mXR7	1.3 ± 0.2	1.8 ± 0.4
RRF/EF-G	RRF (EF-G = 3 μM ; IF3 = 1 μM)	Vacant ribosome	0.18 ± 0.03	3.2 ± 0.4
RRF/EF-G	EF-G (RRF = 5 μM ; IF3 = 1 μM)	Vacant ribosome	0.20 ± 0.04	2.8 ± 0.7
RRF/EF-G	RRF (EF-G = 3 μM ; IF3 = 2 μM)	70S:mXR7:tRNA ^{Phe}	1.7 ± 0.2	9.8 ± 1.3
RRF/EF-G	EF-G (RRF = 5 μM ; IF3 = 2 μM)	70S:mXR7:tRNA ^{Phe}	0.8 ± 0.2	0.9 ± 0.2

All experiments were conducted at 37°C in LS4 buffer containing 4 mM Mg^{2+} .

Roles of IF3 and deacylated tRNA in ribosome splitting by RRF and EF-G

Previous results (Karimi *et al*, 1999; Peske *et al*, 2005) demonstrated that IF3 is not directly involved in the mechanism of RRF/EF-G-dependent ribosome splitting. Indeed, splitting of both vacant and post-termination-like (PTL) ribosomes by RRF and EF-G occurred in the absence and presence of IF3 (Figure 5A and Table IV). Although the apparent rate, Q , for vacant ribosome splitting decreased from 0.95 to 0.22 s^{-1} by inclusion of IF3 in the assay, the actual splitting rate q , as calculated from Equation 1 above, was similar in the presence (0.13 s^{-1}) and absence (0.16 s^{-1}) of IF3. The apparent rate, Q , for splitting of the PTL ribosomes was 2.65 s^{-1} in the absence and 1.65 s^{-1} in the presence of IF3, whereas the corresponding q values were 1.6 and 1.5 s^{-1} , respectively (Table IV). Moreover, the q value of about 1.5 s^{-1} for the PTL ribosomes remained constant, when the IF3 concentration was increased up to 2 μM , and then decreased slightly upon further increase in the IF3 concentration (results not shown). The unchanging q values upon IF3 addition confirm that IF3 did not participate in RRF/EF-G-catalysed ribosome splitting into subunits, but merely blocked subunit re-association (Karimi *et al*, 1999; Peske *et al*, 2005).

To accurately monitor the time course of ribosome splitting in the absence of IF3, the concentration of free Mg^{2+} in the experiments in Figure 5 was reduced from 4 to 3 mM, which also led to faster ribosome splitting (compare Tables I and IV). This effect of Mg^{2+} was corroborated by the experiment in Figure 5A showing that the increase in Mg^{2+} concentration from 3 to 5 mM under otherwise identical conditions decreased the splitting rate q for the 70S·mXR7·tRNA^{Phe} complex from 1.5 to 0.7 s^{-1} .

The rate of splitting of PTL ribosomes depended significantly on the identity of the deacylated tRNA. PTL ribosomes with different mRNAs (Table II) containing tRNA^{Met} in the P site were split at least three-fold more slowly than those containing tRNA^{Phe} (Table V), as illustrated for the mBar and mXR7 cases in Figure 5B. The mRNAs in these PTL ribosomes had different distances between their SD sequences and the Met or Phe codons (mXR8, mXR8_FM) and varying strength of the SD sequences (mXR7, mBar, mSD022) (Table II), which excludes the possibility that peculiarities of an mRNA could account for the slower splitting of the tRNA^{Met}-containing PTL ribosomes. Stoichiometric formation of PTL ribosomes was confirmed for the different types of mRNA and tRNA in control experiments verifying lack of splitting by IF1/IF3 (Figure 5B), typical for the PTL ribosomes (Figure 1B).

A near-complete splitting of PTL ribosomes by RRF/EF-G in the presence of IF3 ($f_{\text{eq}} < 0.08$) justifies the use of the sum of exponentials to fit light-scattering data (see Materials and

methods for details). Figure 5B shows that RRF/EF-G splitting of 70S·mRNA·tRNA complexes with mBar mRNA was distinctly bi-phasic, whereas splitting of complexes with mXR7 mRNA was mainly mono-phasic for both tRNA^{Met} and tRNA^{Phe} (Table V). Distinct bi-phasic splitting by RRF/EF-G was also observed for some complexes formed with mXR8_FM and mSD022 mRNAs. Qualitatively similar bi-phasic behaviour has previously been observed in fast kinetics studies of EF-G-dependent translocation with pre-translocation ribosomes assembled on mSD022-like mRNAs (Peske *et al*, 2004). It was suggested that the slow phase is related to ribosomes with the 30S subunit in inactive conformation and that the fast phase is related to EF-G-dependent translocation on ribosomes with the 30S subunit in active conformation (Peske *et al*, 2004). Accordingly, we suggest that the fast phase is related to RRF/EF-G-dependent splitting of fully active PTL ribosomes. In line with this, we found similar fast phase rate and amplitude for the RRF/G-dependent splitting (Table V) when the PTL ribosomes were prepared by puromycin treatment of 70S·mRNA·fMet-tRNA^{Met} initiation complexes formed in the presence of IFs (see Materials and methods for details). This shows, first, that the bi-phasic behaviour of ribosome splitting was not due to heterogeneity of the 70S·mRNA·tRNA^{Met} complexes caused by mRNAs in different frames (Table II) and, second, that PTL ribosomes prepared by incubation of 70S ribosomes with mRNA and deacylated tRNA were functionally identical to post-termination ribosomes obtained after puromycin-release of the nascent peptide (Peske *et al*, 2005).

Effects of different mRNAs on the rate of ribosome splitting by IF1/IF3

The rate of IF1/IF3-dependent splitting of 70S·mRNA complexes was different for different mRNAs (Figure 5C). The rate correlated well with the strength of the SD sequence, with XR7 mRNA associated with the largest and mSD022 mRNA with the smallest rate (Table V). The splitting rate varied somewhat for mRNAs with the same strong SD sequence (mXR7, mXR8 and mXR8_FM), indicating that sequence elements other than the SD sequence may modulate the IF1/IF3-dependent splitting. Comparisons of the splitting rates for the same 70S·mRNA complexes in Tables I and V show, in addition, that similar to the case of RRF/EF-G-dependent splitting, increasing Mg^{2+} concentration reduces the rate of IF1/IF3-dependent splitting.

Discussion

We have shown that IF1 together with IF3 and RRF together with EF-G have complementary ribosome-splitting activities (Figure 1 and Table I). Ribosome splitting into subunits by

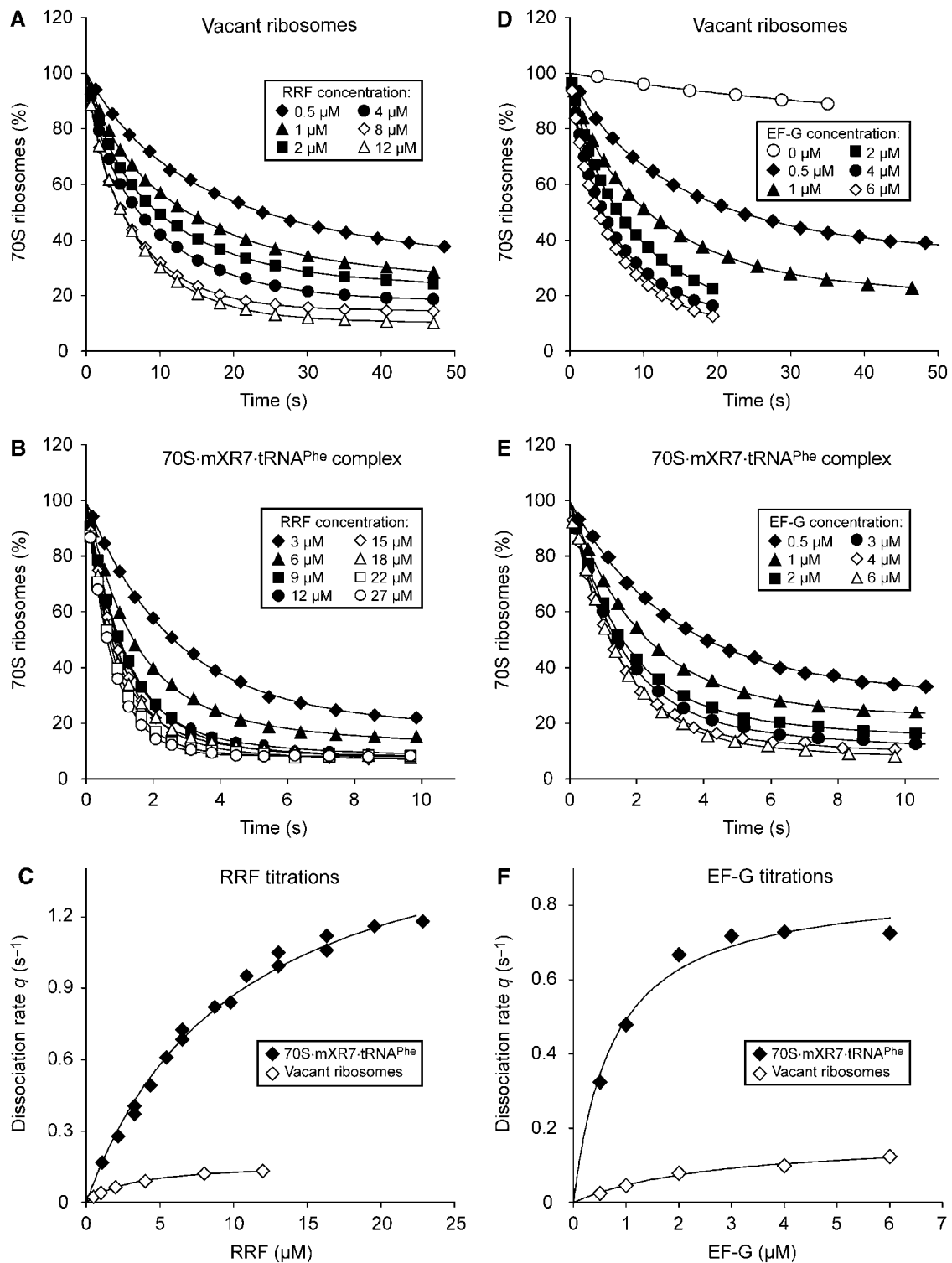


Figure 3 Effects of RRF and EF-G concentrations on the rate of RRF/EF-G-dependent splitting of vacant ribosomes and 70S·mXR7·tRNA^{Phe} complexes. (A, D) Vacant 70S ribosomes (0.2 μM) or (B, E) 0.2 μM 70S ribosomes pre-incubated with 0.4 μM mXR7 mRNA and 0.4 μM tRNA^{Phe} were rapidly mixed with the mixture containing different concentrations of RRF, 3 μM EF-G, 1 μM IF3 (A) or 2 μM IF3 (B) or with the mixture containing different concentrations of EF-G, 5 μM RRF, 1 μM IF3 (D) or 2 μM IF3 (E). All mixtures were prepared in LS4 buffer. (C, F) The splitting rate q plotted versus the concentration, [S], of RRF (C) or EF-G (F) was fitted to the Michaelis–Menten equation $q = q_{\text{cat}}[S]/([S] + K_{\text{M}(S)})$.

IF1/IF3 is fastest for ribosomal complexes containing an mRNA with a strong SD sequence (Figure 1B). At the same time, ribosome splitting by RRF/EF-G is least efficient for such complexes (Figure 1C). Splitting by RRF/EF-G is fastest for PTL ribosomes containing both an mRNA and a

P-site-bound deacylated tRNA (Figure 1C), whereas splitting of such ribosomes by IF1/IF3 is negligible (Figure 1B). We have also found that, in the absence of IF1 and presence of IF3, mRNAs with strong SD sequences increase the ribosome-splitting rate by an order of magnitude

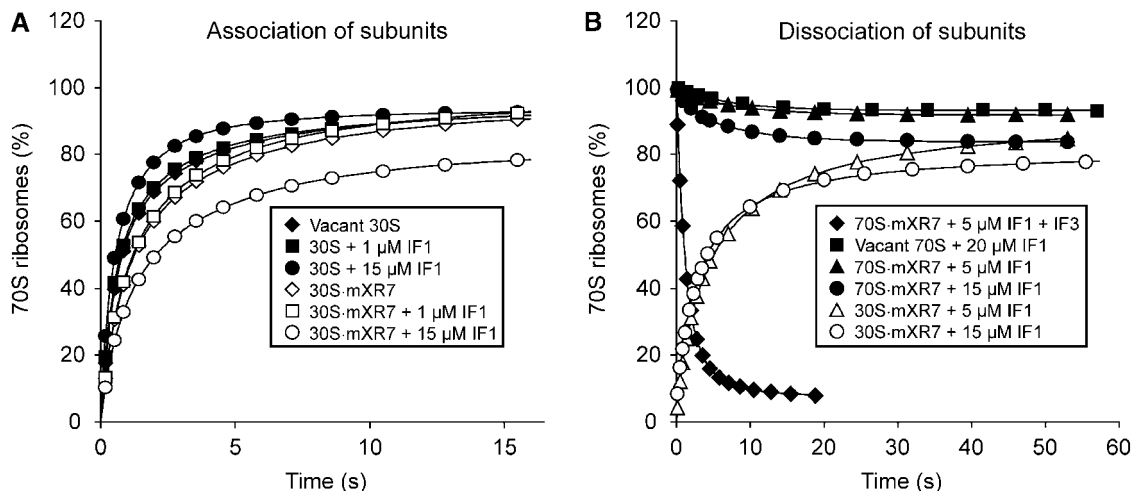


Figure 4 Effects of IF1 on the association/dissociation kinetics of vacant ribosomes or 70S·mRNA complexes. (A) 30S subunits (0.2 μ M) (closed symbols) or 30S·mXR7 complexes (open symbols) containing no IF1 ($\blacklozenge, \blacklozenge$), 1 μ M IF1 (\blacksquare, \square) or 15 μ M IF1 (\bullet, \circ) were mixed with 0.2 μ M 50S subunits. (B) 30S·mRNA complexes (0.2 μ M) containing 5 μ M IF1 (\triangle) or 15 μ M IF1 (\circ) were mixed with 0.2 μ M 50S subunits; 0.2 μ M 70S ribosomes were mixed with 20 μ M IF1 (\blacksquare); 0.2 μ M 70S·mXR7 complexes were mixed with 5 μ M IF1 (\blacktriangle) or 15 μ M IF1 (\bullet) or with 15 μ M IF1 and 2 μ M IF3 (\blacklozenge). All mixtures were prepared in LS3 buffer containing 3 mM free Mg^{2+} .

(Figure 1A). In addition, our results demonstrate that IF1 and IF3 exerts an effect synergistically in the ribosome splitting. IF3 can, in the presence of IF1, bind to vacant ribosomes and 70S·mRNA complexes and promote their rapid splitting into subunits (Figure 4B). We have also demonstrated that PTL ribosomes are split much faster than vacant ribosomes by RRF and EF-G (Figure 1C and Figure 5A), and that the splitting rate depends on the identity of the deacylated tRNA in the P site (Figure 5B).

On the basis of these observations, we propose that ribosome splitting by IF1 with IF3 and by RRF with EF-G occur according to different mechanistic principles. We also propose the existence of a previously unrecognized pathway for ribosome activation in the living cell by the joint actions of mRNA, IF1 and IF3.

On the mechanism of ribosome splitting by IF1 and IF3

Vacant 70S ribosome splitting by IF1 and IF3 has a K_M value for IF1 of about 20 μ M and a q_{cat} value of about 0.35 s^{-1} (Figure 2 and Table III). This large K_M value explains why only a relatively small increase in ribosome splitting-rate was observed previously upon the addition of IF1 and IF3 at low concentrations (Noll and Noll, 1972; Grunberg-Manago *et al*, 1975). This K_M value is also much larger than the equilibrium dissociation constant (K_d) of about 1 μ M for IF1 binding to the free 30S subunit (Zucker and Hershey, 1986; Dahlquist and Puglisi, 2000), suggesting that the 30S subunit changes conformation upon docking with the 50S subunit from a form with high to a form with low affinity to IF1. Conversely, the low affinity of IF1 to the ribosome implies that a new, high-energy conformation of the 30S subunit in the 70S ribosome is induced upon IF1 binding. The existence of such a high-energy conformation of the 30S·IF1 complex is in line with the previous chemical footprinting (Moazed *et al*, 1995; Dahlquist and Puglisi, 2000) and crystallography (Carter *et al*, 2001) observations that the binding of IF1 to the A site of the 30S subunit induces a conformational change of helix 44 of 16S rRNA that may break some of the numerous inter-subunit bridges (Carter *et al*, 2001).

The IF1/IF3-dependent splitting of ribosomal complexes containing mRNAs with strong SD sequences has a much larger q_{cat} ($\sim 1.3 s^{-1}$) and a much smaller $K_{M(IF1)}$ ($\sim 2 \mu$ M) than those for the splitting of vacant ribosomes (Figure 2 and Table III). The reduced K_M value could be due to a stabilization of the high-energy conformation of the 30S subunit in the 70S·IF1 complex by mRNA, which would also account for the larger splitting rate in the presence of mRNA (Tables I and III). Binding of mRNA to a vacant ribosome and formation of the SD·ASD duplex will remove the ASD sequence in 16S rRNA from the P site of the 30S subunit (Wimberly *et al*, 2000; Yusupova *et al*, 2001). Moreover, formation of the SD ASD duplex affects the conformation of the 30S subunit and, in particular, the orientation of its head (Korostelev *et al*, 2007). This could mean that the conformational changes in the 30S subunit triggered by the mRNA-dependent removal of the P-site-bound ASD sequence destabilize the inter-subunit interactions. This scenario would rationalize the observation (Table I and Table V) that mRNAs with strong SD sequences, which, by hypothesis, remove completely the ASD sequence from the P site, accelerate ribosome splitting much more than mRNAs with weak SD sequences, which may only partially remove the P-site-bound ASD sequence.

We have found that IF1 alone induces dissociation of vacant ribosomes and 70S·mRNA complexes into subunits, whereas it affects the rate constants for subunit association only marginally (Figure 4). This refutes the prevailing notion that IF1 equally increases subunit dissociation and association rate constants at an unaltered equilibrium constant K_d (Gualerzi and Pon, 1990; Carter *et al*, 2001). Moreover, we found the dissociation rate constant q for the splitting of 70S·mRNA complexes by IF1 alone to increase 60-fold to one per second upon IF3 addition (Figure 4B). Qualitatively similar effects of IF3 on the IF1-dependent q value are also observed for vacant ribosomes (Figure 4). These results demonstrate that a pure anti-association model of IF3 action, where IF3 does not affect the rate of ribosome splitting into subunits, but only prevents subunit re-association (Grunberg-Manago *et al*, 1975) is untenable in the presence of IF1. The

synergistic effects of IF1 and IF3 on ribosome splitting may, we suggest, be explained by high-affinity binding of IF3 to an IF1-induced high-energy state of the vacant ribosome and of the 70S·mRNA complex. This putative high-energy state could be visualized as a ‘half-opened’ conformation of the 70S ribosome, in which IF3 gains access to its binding site on the 30S subunit (Dallas and Noller, 2001). IF3 binding to this ‘half-opened’ ribosome would block its closure, thereby promoting rapid subunit dissociation.

On the mechanism of ribosome splitting by RRF and EF-G

We have found the maximal ribosome-splitting rate in an RRF titration at constant EF-G concentration to be 10 times larger for PTL ribosomes with an mRNA and a deacylated tRNA in the P site than for vacant ribosomes (Figure 3C and Table III). Authentic post-termination ribosomes are the physiological splitting targets for RRF and EF-G (Janosi *et al*, 1998; Karimi *et al*, 1999), and the present finding that similar PTL ribosomes are split most rapidly by RRF and EF-G may therefore not seem surprising. As, however, PTL ribosomes cannot be opened by IF3 or by IF1/IF3 (Figure 1 and Table I), their rapid opening by RRF/EF-G suggests two very different mechanisms for passive ribosome splitting by IF1 and IF3 on the one hand and active, free energy dissipating (GTP hydrolysis) splitting by RRF and EF-G, on the other. The difference between the mechanisms is further emphasized by the observation that, in contrast to IF1/IF3-dependent splitting, the rate of RRF/EF-G dependent splitting is not affected by IF3 (Figures 4 and 5, and Table IV), and, hence, that IF3 is not involved in the mechanism of RRF/EF-G-dependent ribosome splitting (Karimi *et al*, 1999; Peske *et al*, 2005).

It was reported by Peske *et al* (2005) that vacant ribosomes and post-termination ribosomal complexes are split by RRF/EF-G with similar efficiency. However, we note that the amplitudes and time evolution of the ribosome splitting in their experiments depended strongly on IF3, reminiscent of the present results shown in Figure 5A, implying that the splitting without IF3 was incomplete due to significant re-association of subunits. Under these conditions, it is necessary to disentangle the true rate constant (q) for dissociation of the 70S ribosome from the observed relaxation rate (Q) as in Equation (1), and it is not clear that this was done by Peske *et al*. The apparent discrepancy between our results may

therefore be removed by taking into account the subunit re-association in the evaluation of their ribosome-splitting data.

The K_M values for EF-G and RRF in the splitting of vacant ribosomes (Table III) are more similar to the K_d values for EF-G (1.3 μ M) and RRF (3.0 μ M) binding to the ribosome at excess concentration of the other factor than to the corresponding K_d values for EF-G (0.055 μ M) and RRF (0.13 μ M) in the absence of the other factor (Seo *et al*,

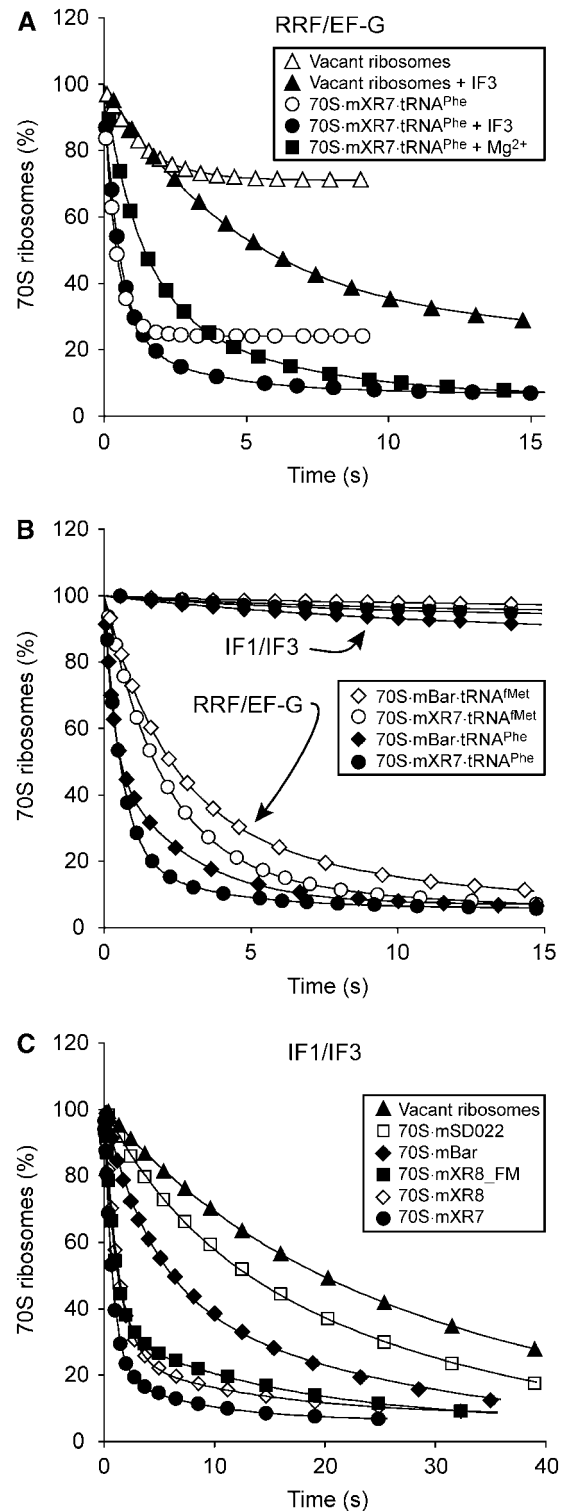


Figure 5 Effects of IF3, Mg²⁺, mRNA and tRNA identity on the ribosomal splitting by RRF/EF-G and IF1/IF3. (A) Mixture 1 containing 0.2 μ M vacant 70S ribosomes (\triangle , \blacktriangle) or 0.2 μ M 70S ribosomes pre-incubated with 0.5 μ M mXR7 mRNA and 0.4 μ M deacylated tRNA^{Phe} (\circ , \bullet , \blacksquare) was rapidly mixed with mixture 2 containing 9 μ M RRF, 4 μ M EF-G and no IF3 (open symbols) or 0.3 μ M IF3 (closed symbols). (B) Mixture 1 containing 0.2 μ M 70S ribosomes pre-incubated with 0.5 μ M of mXR7 (\bullet , \circ) or mBar (\blacklozenge , \diamond) mRNAs together with 0.4 μ M tRNA^{Phe} (closed symbols) or 0.4 μ M tRNA^{Met} (open symbols) was rapidly mixed with mixture 2 containing 9 μ M RRF, 4 μ M EF-G and 0.3 μ M IF3 or with mixture 2 containing 15 μ M IF1 and 2 μ M IF3. (C) Mixture 1 containing 0.2 μ M vacant 70S ribosomes (\blacktriangle), 0.2 μ M 70S ribosomes pre-incubated with 0.5 μ M of mSD022 (\square), mBar (\blacklozenge), mXR8_{FM} (\blacksquare), mXR8 (\diamond) or mXR7 (\bullet) mRNAs was rapidly mixed with mixture 2 containing 5 μ M IF1 and 2 μ M IF3. All mixtures were prepared in LS3 buffer, except that experiment marked (\blacksquare) in (A) was conducted in LS5 buffer containing 5 mM free Mg²⁺.

Table IV Effect of IF3 on the RRF/EF-G-dependent splitting of vacant ribosomes and 70S·mXR7·tRNA^{Phe} complexes

	f_{eq}	Q (s ⁻¹)	q (s ⁻¹)
Vacant 70S ribosome (-IF3)	0.7	0.95 ± 0.08	0.16 ± 0.04
Vacant 70S ribosome (+IF3)	0.25	0.22 ± 0.02	0.13 ± 0.01
70S·mXR7·tRNA ^{Phe} (-IF3)	0.24	2.65 ± 0.08	1.60 ± 0.05
70S·mXR7·tRNA ^{Phe} (+IF3)	0.05	1.65 ± 0.07	1.51 ± 0.06

Apparent rate of ribosome splitting, Q , was obtained from nonlinear regression fit of experimental data to the relation $I(t) = A_1 \frac{(1+f_{eq})\exp(-Qt)}{1+f_{eq}\exp(-Qt)} + A_{BKG}$ (Equation (8) in Materials and methods) after which q was calculated from Equation (1). All experiments were conducted at 37°C in LS3 buffer containing 3 mM Mg²⁺.

2004). This is in line with the notion that ribosome splitting requires the simultaneous presence of both factors on the ribosome (Seo *et al*, 2004).

Ribosome splitting occurs in response to EF-G binding to RRF containing 70S ribosomes, and requires both GTP bound to EF-G and GTP hydrolysis (Karimi *et al*, 1999; Peske *et al*, 2005; Zavialov *et al*, 2005b). Cryo-EM studies of a post-termination ribosome have shown that RRF is bound to the ratcheted conformation of the ribosome with the deacylated tRNA in hybrid P/E site (Gao *et al*, 2005; Barat *et al*, 2007). In contrast, RRF is bound to a non-ratcheted conformation of a vacant ribosome, both according to cryo-EM (Agrawal *et al*, 2004; Barat *et al*, 2007) and crystallographic (Pai *et al*, 2008) studies, and to a non-ratcheted conformation of a ribosome in complex with mRNA and an anticodon stem loop analogue of tRNA (ASL) in the P site (Weixlbaumer *et al*, 2007). Taken together, these structural results may provide a simple explanation for the accelerated RRF/EF-G splitting of the ribosome and the increased K_M value for RRF action (Table III) as conferred by the presence of a deacylated full-length tRNA on the ribosome. That is, as the binding site of RRF overlaps with the P site on the 50S subunit (Weixlbaumer *et al*, 2007), we propose that on the 70S ribosome RRF can coexist with a deacylated tRNA in the P/E but not in the P/P site, which explains why RRF binding drives the post-termination but neither the vacant nor the ASL-bound ribosome to the ratcheted state. Subsequent binding of EF-G to the ratcheted ribosome and GTP hydrolysis induce rotation of domain II of RRF towards the S12 protein and H44 helix of the 30S subunit, thereby disrupting the B2a and B3 inter-subunit bridges and, eventually, splitting the ribosome (Gao *et al*, 2005, 2007). In the cases of vacant or ASL-bound ribosomes, RRF can bind to the non-ratcheted ribosome with high affinity, which explains both the small rate and the small K_M value for RRF splitting of the vacant ribosome (Table III). As EF-G in the GTP form has highest affinity to the ratcheted ribosome (Zavialov *et al*, 2005a), this would also explain a lower K_M value for EF-G when the factor enters a ratcheted RRF-bound post-termination complex than when it enters a non-ratcheted RRF-bound vacant ribosome (Table III). In this view, splitting of the post-termination and the vacant ribosomes have the RRF-bound ratcheted ribosome as a common intermediate, favoured by the presence of a deacylated tRNA in the post-termination ribosome.

We have also observed that the RRF/EF-G-dependent ribosome-splitting rate is sensitive to the identity of the deacylated tRNA in the P site, that is, decreasing from 1.8 to 0.5 s⁻¹ upon substitution of tRNA^{Phe} for tRNA^{Met} in the

Table V Effects of mRNA and tRNA identity on the splitting of ribosomal complexes by RRF/EF-G and IF1/IF3

Splitting by RRF/EF-G	A_1 (%)	q_1 (s ⁻¹)	A_2 (%)	q_2 (s ⁻¹)
<i>70S:mRNA:tRNA^{Phe} with</i>				
mXR7	85	1.77 ± 0.06	15	0.33 ± 0.03
mXR8	81	1.72 ± 0.06	19	0.32 ± 0.03
mXR8_FM	78	1.44 ± 0.05	22	0.33 ± 0.04
mBar	55	2.8 ± 0.08	45	0.31 ± 0.05
mSD022	65	1.47 ± 0.06	35	0.29 ± 0.04
<i>70S:mRNA:tRNA^{Met} with</i>				
mXR7	88	0.51 ± 0.02	12	0.12 ± 0.03
mXR8	85	0.48 ± 0.02	15	0.13 ± 0.02
mXR8_FM	47	0.47 ± 0.05	53	0.18 ± 0.03
mBar	73	0.48 ± 0.03	27	0.11 ± 0.02
mSD022	71	0.51 ± 0.03	29	0.15 ± 0.03
<i>70S:mRNA:tRNA^{Met} prepared from initiation complexes with</i>				
mXR7	92	0.54 ± 0.02	8	0.09 ± 0.02
mXR8	86	0.51 ± 0.02	14	0.08 ± 0.02
mXR8_FM	55	0.41 ± 0.04	45	0.08 ± 0.03
mBar	64	0.50 ± 0.04	36	0.11 ± 0.03
mSD022	81	0.48 ± 0.03	19	0.09 ± 0.02
Splitting by IF1/IF3	A_1	q_1 (s ⁻¹)	A_2	q_2 (s ⁻¹)
70S	81	0.07 ± 0.03	19	0.03 ± 0.005
70S:mXR7	87	1.23 ± 0.06	13	0.08 ± 0.02
70S:mXR8	83	0.81 ± 0.05	17	0.07 ± 0.01
70S:mXR8_FM	76	1.05 ± 0.06	24	0.06 ± 0.01
70S:mBar	59	0.28 ± 0.04	41	0.05 ± 0.02
70S:mSD022	80	0.11 ± 0.03	20	0.04 ± 0.005

Parameters A_1 , A_2 , q_1 and q_2 were determined from nonlinear regression fit of experimental data to the relation $I(t) = A_1 \exp(-q_1 t) + A_2 \exp(-q_2 t) + A_{BKG}$ (Equation (10) in Materials and methods). All experiments were conducted at 37°C in LS3 buffer containing 3 mM Mg²⁺.

70S·mRNA·tRNA complex (Figure 5B and Table V). This tRNA-dependent decrease in the splitting rate is observed for different mRNAs (Table II), suggesting that it is related to the tRNA, rather than the mRNA, identity. Recent fast kinetics data demonstrate that the first step in EF-G-driven translocation is movement of the P/P site tRNA to the hybrid P/E site (Pan *et al*, 2007) and, by inference, movement of the ribosome into the ratcheted state. Interestingly, the rate of this tRNA movement is sensitive to tRNA modifications (Pan *et al*, 2007), suggesting that also the identity of the deacylated tRNA may affect either the stability of, or the rate of attaining, the ratcheted ribosomal conformation in the presence of RRF. Either one of these effects could then account for the observed difference in the rate of splitting of post-termination complexes with different deacylated tRNAs (Table V).

When EF-G enters the post-termination ribosome, the presence of RRF, instead of an A-site-bound peptidyl-tRNA, blocks the second step of translocation, in which the mRNA moves by one codon and the deacylated tRNA moves from the P site of the 30S subunit to the E site and out from the ribosome (Karimi *et al*, 1999; Peske *et al*, 2005). This may also explain why antibiotic drugs, such as spectinomycin and viomycin, that specifically block the tRNA·mRNA translocation on the 30S subunit (Peske *et al*, 2004; Pan *et al*, 2007) have a very small effect on the RRF/EF-G-dependent ribosome-splitting reaction (MYP, unpublished results).

Two complementary ribosome-splitting pathways in the living cell

We have found that RRF, together with EF-G, splits PTL ribosomes and that IF1, together with IF3, splits ribosomes containing mRNAs with strong SD sequences with rates superseding one per second (Tables III–V). Interestingly, the rate of the RRF/EF-G splitting of the 70S·mBar·tRNA^{Phe} complex formed with mBar mRNA with a weak SD sequence exceeds 2 s^{-1} (Table V), indicating that splitting into subunits of the authentic post-termination ribosome with no SD sequence at all may be even faster. From these observations, we suggest that there exist two physiologically relevant ribosome-splitting pathways in the bacterial cell. Their relevance is further corroborated by the fact that the K_M values for the corresponding reactions (Table III) are well below the total concentrations of RRF (20 μM) (Andersen *et al*, 1999; Seo *et al*, 2004) and IF1 (8–12 μM) (Howe and Hershey, 1983) in the cytoplasm of the *E. coli* cell.

Splitting of post-termination ribosomes by RRF and EF-G is the major route for continuous supply of ribosomal subunits for new initiation events to sustain stable protein synthesis in the cell (Janosi *et al*, 1996; Kisselev *et al*, 2003), which explains why RRF is essential in bacteria (Janosi *et al*, 1998). However, there exist other than post-termination ribosomal complexes in the cell, and these must eventually become available for initiation of protein synthesis in a regulated manner. For instance, bacterial cells in poor media have a large pool of vacant ribosomes stored in an inactive state either as 70S ribosomes in complex with the YfiA protein (Vila-Sanjurjo *et al*, 2004; Ueta *et al*, 2005) or as 100S dimers in complexes with the RMF and YhbH proteins (Ueta *et al*, 2005). When, however, the quality of the medium improves, these ribosomes must rapidly become activated for rapid resumption of protein elongation (Vila-Sanjurjo *et al*, 2004; Ueta *et al*, 2005). We suggest that the greatly increased mRNA availability (Kuzj *et al*, 1998) and rate of mRNA synthesis that accompany up-shifts from poor to rich growth media (Liang *et al*, 2000) induce massive mRNA binding to such inactive ribosomes, which then leads to their rapid splitting into subunits by the cooperative action of IF1 and IF3 (Figure 1 and Table I). As we have shown here, different mRNAs may accelerate IF1/IF3-dependent ribosome splitting very differently (Figure 5C and Table V). Stored ribosomes may therefore be re-activated preferentially by splitting-efficient mRNAs, which may lead to preferential expression of proteins encoded by such mRNAs during transition from stationary to exponential growth phase.

There will also be a pool of mRNA-bound, tRNA-less 70S ribosomes during growth in high-quality media, due to either aberrant (Menninger, 1976) or programmed peptidyl-tRNA drop-off, as recently found in regulation of *trp* operon expression (Gong *et al*, 2007). Such drop-off events are likely to occur during translation of the very first codons of mRNAs (Heurgue-Hamard *et al*, 2000; Gonzalez de Valdivia and Isaksson, 2005), allowing for re-formation of the initial SD-ASD interaction by ribosomal back-sliding on the mRNA (Pavlov *et al*, 1997), after which the 70S·mRNA complex can be efficiently split by IF1/IF3.

From these considerations, we propose that IF1, in addition to its well-established roles as enhancer of the rate (Gualerzi and Pon, 1990; Antoun *et al*, 2006b) and accuracy (Antoun *et al*, 2006a) of initiation of protein synthesis, is

essential for rapid recovery of ribosomal complexes during up-shifts in the growth medium as well as after peptidyl-tRNA drop-off during steady-state growth.

Materials and methods

Chemicals and buffers

tRNA^{fMet}, tRNA^{Phe}, phosphoenolpyruvate (PEP), myokinase (MK), pyruvate kinase (PK), putrescine and spermidine were from Sigma (USA). Experiments were conducted in a polymix-like buffer, LS3, containing 95 mM KCl, 5 mM NH₄Cl, 0.5 mM CaCl₂, 8 mM putrescine, 1 mM spermidine, 30 mM HEPES pH 7.5, 1 mM DTE, 2 mM PEP, 1 mM GTP, 1 mM ATP and 5 mM Mg(OAc)₂, supplemented with 1 $\mu\text{g/ml}$ PK and 0.1 $\mu\text{g/ml}$ MK (Jelenc and Kurland, 1979). As each ATP or GTP molecule chelate one Mg²⁺ cation, the free Mg²⁺ concentration in the LS3 buffer was assumed to be 3 mM. The concentration of free Mg²⁺ in the LS4 and LS5 buffers was adjusted by adding 1 or 2 mM Mg(OAc)₂ to the LS3 buffer.

Components of the translation system

Synthetic mRNAs with the sequences compiled in Table II were prepared according to Pavlov *et al* (1997). 70S ribosomes, 50S and 30S subunits, [³H]fMet-tRNA^{fMet}, IFs, elongation factors and RRF were prepared as described in Freistroffer *et al* (1997); Antoun *et al* (2006b).

Dissociation of ribosomal complexes into subunits

Two mixtures, 1 and 2, were prepared in the LS buffer of indicated Mg²⁺ concentration. Mixture 1 contained 70S ribosomes and, when indicated, mRNA, deacylated tRNA^{Phe} or tRNA^{fMet} in concentrations specified for each experiment. Mixture 2 contained IF3 and, when indicated IF1, RRF, EF-G or mRNA in concentrations specified for each experiment. Both mixtures were pre-incubated for 20 min at 37°C and loaded in the syringes of a stopped-flow instrument (SX-20; Applied Photophysics, Leatherhead, UK). The kinetics of dissociation of 70S ribosomes into subunits was monitored at 37°C with light scattering after rapid mixing equal volumes of mixtures 1 and 2 as described (Antoun *et al*, 2006b).

Alternatively, mixture 1 containing 70S·mRNA·tRNA^{fMet} complexes was prepared as follows. First, 70S ribosomes (0.4 μM) were pre-incubated with indicated mRNA (1 μM), IF1 (0.5 μM), IF2 (0.5 μM) and IF3 (0.5 μM) for 10 min at 37°C after which fMet-tRNA^{fMet} (0.4 μM) was added and the incubation was continued for 5 more minutes. Before loading into the syringe of the stopped-flow instrument 0.1 mM puromycin was added to mixture 1 and the incubation was continued for 10 more minutes at 37°C before rapid mixing with mixture 2. The formation of 70S initiation complexes was confirmed by the dipeptide formation assay (Antoun *et al*, 2006b) and by the absence of the splitting by RRF/EF-G when the puromycin treatment was omitted (Peske *et al*, 2005).

Treatment of light scattering data

It can be shown (see Supplementary data) that the time course of the 70S concentration, $r(t)$, for the kinetic scheme (2) is given by:

$$\frac{r(t) - r_{\text{eq}}}{r_0 - r_{\text{eq}}} = \frac{I(t) - I_{\text{eq}}}{I_0 - I_{\text{eq}}} = \frac{\exp(-Qt)}{1 - ((r_0 - r_{\text{eq}})/g)(1 - \exp(-Qt))} \quad (3)$$

where r_0 is the initial and r_{eq} is the steady state or equilibrium concentration of 70S ribosomes, I_0 and I_{eq} are the corresponding light scattering intensities (Antoun *et al*, 2006b). The parameter g in Equation (3) is

$$g = [30\text{S}]_{\text{eq}} + [50\text{S}]_{\text{eq}} + \frac{q}{k} = [30\text{S}]_{\text{eq}} + [50\text{S}]_{\text{eq}} + K_d \quad (4)$$

whereas the apparent rate Q is

$$Q = kg = q + k([30\text{S}]_{\text{eq}} + [50\text{S}]_{\text{eq}}) = q \left(1 + \frac{[30\text{S}]_{\text{eq}} + [50\text{S}]_{\text{eq}}}{K_d} \right) \quad (5)$$

In dissociation experiments, one starts with non-dissociated 70S ribosomes. Therefore

$$[30\text{S}]_{\text{eq}} = [50\text{S}]_{\text{eq}} = r_0 - r_{\text{eq}}$$

which allows one to re-write Equation (5) for Q as

$$Q = q \left(1 + 2 \frac{r_0 - r_{eq}}{K_d} \right) = q \left(1 + 2 \frac{r_0 - r_{eq}}{(r_0 - r_{eq})^2} r_{eq} \right) = q \frac{r_0 + r_{eq}}{r_0 - r_{eq}}$$

or

$$Q = q \frac{1 + f_{eq}}{1 - f_{eq}} = kK_d \frac{1 + f_{eq}}{1 - f_{eq}} = kr_0 \frac{1 - f_{eq}^2}{f_{eq}} \quad (6)$$

Here, we introduced the fraction f_{eq} of non-dissociated 70S ribosomes in equilibrium

$$f_{eq} = \frac{r_{eq}}{r_0}$$

and used the definition of the equilibrium dissociation constant

$$K_d = \frac{q}{k} = \frac{[30S]_{eq}[50S]_{eq}}{[70S]_{eq}} = \frac{(r_0 - r_{eq})^2}{r_{eq}} = r_0 \frac{(1 - f_{eq})^2}{f_{eq}} \quad (7)$$

Using Equations (6) and (7) one can re-write general Equation (3) for the case of ribosomal dissociation as:

$$\begin{aligned} \frac{I(t) - I_{eq}}{I_0 - I_{eq}} &= \frac{\exp(-Qt)}{1 - (f_{eq}/(1 + f_{eq}))(1 - \exp(-Qt))} \\ &= \frac{(1 + f_{eq}) \exp(-Qt)}{1 + f_{eq} \exp(-Qt)} \end{aligned} \quad (8)$$

The apparent dissociation rate Q can be obtained by nonlinear fit of experimental light scattering data to relation (8). This fit can be made more reliable by an independent estimate of f_{eq} obtained from properly normalized scattering intensities (Antoun *et al*, 2006b). The actual dissociation rate q is then calculated from Q using Equation (6) or equivalent Equation (1). It can also be shown that when $f_{eq} < 0.1$ the q values estimated by first calculating Q by a nonlinear fit of experimental data to Equation (8) and then by using Equation (1) are very close

References

- Agrawal RK, Sharma MR, Kiel MC, Hirokawa G, Booth TM, Spahn CM, Grassucci RA, Kaji A, Frank J (2004) Visualization of ribosome-recycling factor on the *Escherichia coli* 70S ribosome: functional implications. *Proc Natl Acad Sci USA* **101**: 8900–8905
- Andersen LD, Moreno JM, Clark BF, Mortensen KK, Sperling-Petersen HU (1999) Immunochemical determination of cellular content of translation release factor RF4 in *Escherichia coli*. *IUBMB Life* **48**: 283–286
- Antoun A, Pavlov MY, Lovmar M, Ehrenberg M (2006a) How initiation factors maximize the accuracy of tRNA selection in initiation of bacterial protein synthesis. *Mol Cell* **23**: 183–193
- Antoun A, Pavlov MY, Lovmar M, Ehrenberg M (2006b) How initiation factors tune the rate of initiation of protein synthesis in bacteria. *EMBO J* **25**: 2539–2550
- Barat C, Datta PP, Raj VS, Sharma MR, Kaji H, Kaji A, Agrawal RK (2007) Progression of the ribosome recycling factor through the ribosome dissociates the two ribosomal subunits. *Mol Cell* **27**: 250–261
- Benne R, Ebes F, Voorma HO (1973) Sequence of events in initiation of protein synthesis. *Eur J Biochem* **38**: 265–273
- Carter AP, Clemons Jr WM, Brodersen DE, Morgan-Warren RJ, Hartsch T, Wimberly BT, Ramakrishnan V (2001) Crystal structure of an initiation factor bound to the 30S ribosomal subunit. *Science* **291**: 498–501
- Dahlquist KD, Puglisi JD (2000) Interaction of translation initiation factor IF1 with the *E. coli* ribosomal A site. *J Mol Biol* **299**: 1–15
- Dallas A, Noller HF (2001) Interaction of translation initiation factor 3 with the 30S ribosomal subunit. *Mol Cell* **8**: 855–864
- Freistoffer DV, Pavlov MY, MacDougall J, Buckingham RH, Ehrenberg M (1997) Release factor RF3 in *E. coli* accelerates the dissociation of release factors RF1 and RF2 from the ribosome in a GTP-dependent manner. *EMBO J* **16**: 4126–4133

to those obtained by a direct fit of experimental data to an exponential equation:

$$I(t) = (I_0 - I_{eq}) \exp(-qt) + I_{eq} = A_1 \exp(-qt) + A_0 \quad (9)$$

We used therefore Equation (9) in the cases when ribosome dissociation was close to completion ($f_{eq} < 0.1$). In some of such cases a double exponential fit of experimental data according to

$$I(t) = A_1 \exp(-q_1 t) + A_2 \exp(-q_2 t) + A_0 \quad (10)$$

was clearly better than according to Equation (9).

For the case of the association of 30S and 50S subunits when their total concentrations are equal the general expression (3) becomes (see Supplementary data for details):

$$\frac{I(t) - I_{eq}}{I(0) - I_{eq}} = \frac{(1 - f_{eq}^2) \exp(-Qt)}{1 - f_{eq}^2 \exp(-Qt)} \quad (11)$$

This relation together with relation (1) was used to calculate the association rate constants in experiments in Figure 4.

The fit of experimental data to Equations (8)–(11) to obtain Q or q parameters and their standard deviations was carried out using the nonlinear regression program Origin 7 (OriginLab Corp.). The original light scattering traces were used to calculate all kinetic parameters in Tables I, III–V. However, for clarity of presentation we used a digital filter to reduce the noise and the numbers of data points in the figures.

Supplementary data

Supplementary data are available at *The EMBO Journal* Online (<http://www.embojournal.org>).

Acknowledgements

We thank Drs Joachim Frank and Ning Gao for their valuable comments on the paper. This study was supported by the Swedish Research Council, NIH (GM70768) and the Egyptian mission department.

- Gao N, Zavialov AV, Ehrenberg M, Frank J (2007) Specific interaction between EF-G and RRF and its implication for GTP-dependent ribosome splitting into subunits. *J Mol Biol* **374**: 1345–1358
- Gao N, Zavialov AV, Li W, Sengupta J, Valle M, Gursky RP, Ehrenberg M, Frank J (2005) Mechanism for the disassembly of the posttermination complex inferred from cryo-EM studies. *Mol Cell* **18**: 663–674
- Gong M, Cruz-Vera LR, Yanofsky C (2007) Ribosome recycling factor and release factor 3 action promotes TnaC-peptidyl-tRNA dropoff and relieves ribosome stalling during tryptophan induction of tna operon expression in *Escherichia coli*. *J Bacteriol* **189**: 3147–3155
- Gonzalez de Valdivia EI, Isaksson LA (2005) Abortive translation caused by peptidyl-tRNA drop-off at NGG codons in the early coding region of mRNA. *FEBS J* **272**: 5306–5316
- Grunberg-Manago M, Dessen P, Pantaloni D, Godefroy-Colburn T, Wolfe AD, Dondon J (1975) Light-scattering studies showing the effect of initiation factors on the reversible dissociation of *Escherichia coli* ribosomes. *J Mol Biol* **94**: 461–478
- Gualerzi CO, Pon CL (1990) Initiation of mRNA translation in prokaryotes. *Biochemistry* **29**: 5881–5889
- Heurgue-Hamard V, Dinckas V, Buckingham RH, Ehrenberg M (2000) Origins of minigene-dependent growth inhibition in bacterial cells. *EMBO J* **19**: 2701–2709
- Howe JG, Hershey JW (1983) Initiation factor and ribosome levels are coordinately controlled in *Escherichia coli* growing at different rates. *J Biol Chem* **258**: 1954–1959
- Janosi L, Hara H, Zhang S, Kaji A (1996) Ribosome recycling by ribosome recycling factor (RRF)—an important but overlooked step of protein biosynthesis. *Adv Biophys* **32**: 121–201
- Janosi L, Mottagui-Tabar S, Isaksson LA, Sekine Y, Ohtsubo E, Zhang S, Goon S, Nelken S, Shuda M, Kaji A (1998) Evidence

- for *in vivo* ribosome recycling, the fourth step in protein biosynthesis. *EMBO J* **17**: 1141–1151
- Jelenc PC, Kurland CG (1979) Nucleoside triphosphate regeneration decreases the frequency of translation errors. *Proc Natl Acad Sci USA* **76**: 3174–3178
- Karimi R, Pavlov MY, Buckingham RH, Ehrenberg M (1999) Novel roles for classical factors at the interface between translation termination and initiation. *Mol Cell* **3**: 601–609
- Kisselev L, Ehrenberg M, Frolova L (2003) Termination of translation: interplay of mRNA, rRNAs and release factors? *EMBO J* **22**: 175–182
- Korostelev A, Trakhanov S, Asahara H, Laurberg M, Lancaster L, Noller HF (2007) Interactions and dynamics of the Shine Dalgarno helix in the 70S ribosome. *Proc Natl Acad Sci USA* **104**: 16840–16843
- Kuzj AE, Medberry PS, Schottel JL (1998) Stationary phase, amino acid limitation and recovery from stationary phase modulate the stability and translation of chloramphenicol acetyltransferase mRNA and total mRNA in *Escherichia coli*. *Microbiology* **144** (Part 3): 739–750
- La Teana A, Pon CL, Gualerzi CO (1993) Translation of mRNAs with degenerate initiation triplet AUU displays high initiation factor 2 dependence and is subject to initiation factor 3 repression. *Proc Natl Acad Sci USA* **90**: 4161–4165
- Liang ST, Xu YC, Dennis P, Bremer H (2000) mRNA composition and control of bacterial gene expression. *J Bacteriol* **182**: 3037–3044
- Menninger JR (1976) Peptidyl transfer RNA dissociates during protein synthesis from ribosomes of *Escherichia coli*. *J Biol Chem* **251**: 3392–3398
- Moazed D, Samaha RR, Gualerzi C, Noller HF (1995) Specific protection of 16S rRNA by translational initiation factors. *J Mol Biol* **248**: 207–210
- Noll M, Noll H (1972) Mechanism and control of initiation in the translation of R17 RNA. *Nat New Biol* **238**: 225–228
- Ontiveros C, Valadez JG, Hernandez J, Guarneros G (1997) Inhibition of *Escherichia coli* protein synthesis by abortive translation of phage lambda minigenes. *J Mol Biol* **269**: 167–175
- Pai RD, Zhang W, Schuwirth BS, Hirokawa G, Kaji H, Kaji A, Cate JH (2008) Structural insights into ribosome recycling factor interactions with the 70S ribosome. *J Mol Biol* **376**: 1334–1347
- Pan D, Kirillov SV, Cooperman BS (2007) Kinetically competent intermediates in the translocation step of protein synthesis. *Mol Cell* **25**: 519–529
- Pavlov MY, Freistoffer DV, MacDougall J, Buckingham RH, Ehrenberg M (1997) Fast recycling of *Escherichia coli* ribosomes requires both ribosome recycling factor (RRF) and release factor RF3. *EMBO J* **16**: 4134–4141
- Peske F, Rodnina MV, Wintermeyer W (2005) Sequence of steps in ribosome recycling as defined by kinetic analysis. *Mol Cell* **18**: 403–412
- Peske F, Savelsbergh A, Katunin VI, Rodnina MV, Wintermeyer W (2004) Conformational changes of the small ribosomal subunit during elongation factor G-dependent tRNA–mRNA translocation. *J Mol Biol* **343**: 1183–1194
- Seo HS, Kiel M, Pan D, Raj VS, Kaji A, Cooperman BS (2004) Kinetics and thermodynamics of RRF, EF-G, and thiostrepton interaction on the *Escherichia coli* ribosome. *Biochemistry* **43**: 12728–12740
- Singh NS, Varshney U (2004) A physiological connection between tmRNA and peptidyl-tRNA hydrolase functions in *Escherichia coli*. *Nucleic Acids Res* **32**: 6028–6037
- Tenson T, Lovmar M, Ehrenberg M (2003) The mechanism of action of macrolides, lincosamides and streptogramin B reveals the nascent peptide exit path in the ribosome. *J Mol Biol* **330**: 1005–1014
- Ueta M, Yoshida H, Wada C, Baba T, Mori H, Wada A (2005) Ribosome binding proteins YbhH and YfiA have opposite functions during 100S formation in the stationary phase of *Escherichia coli*. *Genes Cells* **10**: 1103–1112
- Vila-Sanjurjo A, Schuwirth BS, Hau CW, Cate JH (2004) Structural basis for the control of translation initiation during stress. *Nat Struct Mol Biol* **11**: 1054–1059
- Weixlbaumer A, Petry S, Dunham CM, Selmer M, Kelley AC, Ramakrishnan V (2007) Crystal structure of the ribosome recycling factor bound to the ribosome. *Nat Struct Mol Biol* **14**: 733–737
- Wimberly BT, Brodersen DE, Clemons Jr WM, Morgan-Warren RJ, Carter AP, Vornrhein C, Hartsch T, Ramakrishnan V (2000) Structure of the 30S ribosomal subunit. *Nature* **407**: 327–339
- Yusupova GZ, Yusupov MM, Cate JH, Noller HF (2001) The path of messenger RNA through the ribosome. *Cell* **106**: 233–241
- Zavialov AV, Haurlyiuk VV, Ehrenberg M (2005a) Guanine-nucleotide exchange on ribosome-bound elongation factor G initiates the translocation of tRNAs. *J Biol* **4**: 9
- Zavialov AV, Haurlyiuk VV, Ehrenberg M (2005b) Splitting of the posttermination ribosome into subunits by the concerted action of RRF and EF-G. *Mol Cell* **18**: 675–686
- Zucker FH, Hershey JW (1986) Binding of *Escherichia coli* protein synthesis initiation factor IF1 to 30S ribosomal subunits measured by fluorescence polarization. *Biochemistry* **25**: 3682–3690